The FASEB Journal • Research Communication

A novel eGFP-expressing immunodeficient mouse model to study tumor-host interactions

Simone P. Niclou,*,[1] Claude Danzeisen,* Hans P. Eikesdal,[§] Helge Wiig,[§] Nicolaas H. C. Brons,[†] Aurélie M. F. Poli,[‡] Agnete Svendsen,[§] Anja Torsvik,[§] Per Øyvind Enger,[§] Jorge A. Terzis,* and Rolf Bjerkvig*,[§]

*NorLux Neuro-Oncology Laboratory, [†]Core Facility Flowcytometry, and [‡]Laboratoire d'Immunogénétique et d'Allergologie (LIGA), Centre de Recherche Public de la Santé (CRP-Santé), Luxembourg; and [§]Department of Biomedicine, University of Bergen, Bergen, Norway

ABSTRACT **A NOD/Scid mouse expressing enhanced green fluorescent protein (eGFP) is described, in which human and mouse tumors marked with red fluorescent protein can be established *in vivo*, both at subcutaneous and orthotopic locations. Using light microscopy as well as multiphoton confocal microscopy techniques, we visualized in detail the intricate colocalization of tumor and host cells *in situ*. Moreover, using fluorescence-activated cell sorting (FACS), we were able to completely separate the host cells from the tumor cells, thus providing a system for detailed cellular and molecular analysis of tumor-host cell interactions. The fact that tumor and host cells can be reliably identified also allowed us to detect double-positive cells, possibly arising from cell fusion events or horizontal gene transfer. Similarly, the model can be applied for the detection of circulating metastatic cells and for detailed studies on the vascular compartments within tumors, including vasculogenic mimicry. Thus, the model described should provide significant insight into how tumor cells communicate with their microenvironment.—Niclou, S. P., Danzeisen, C., Eikesdal, H. P., Wiig, H., Brons, N. H. C., Poli, A. M. F., Svendsen, A., Torsvik, A., Enger, P. Ø., Terzis, J. A., Bjerkvig, R. A novel eGFP-expressing immunodeficient mouse model to study tumor-host interactions. *FASEB J.* 22, 3120–3128 (2008)**

Key Words: xenograft · in vivo imaging · vascular mimicry · cell fusion · tumor microenvironment · glioma

NUMEROUS HOST-DERIVED SIGNALING molecules are known to have instructive roles in tumor promotion and suppression, resulting in a complex crosstalk between tumor and various stromal cells (1–3). The strong impact of the microenvironment on tumor development is indicated, *e.g.*, by tumor metastasis to preferential organs and by the occurrence of tumor dormancy (4, 5). The stromal compartments within tumors comprise a variety of cells, including endothelial cells, fibroblasts, and inflammatory cells. Host cells infiltrate and interact with tumor cells, and each of the cell types involved has the potential to influence other cells within the microenvironment through secretion of a large number of growth-stimulating and inhibitory factors, including cytokines (6, 7), proteases and their inhibitors (8), and cell adhesion molecules, as well as extracellular matrix components (9) that stimulate tumor angiogenesis, growth, and metastasis. This complex interplay is extremely difficult to model in *in vitro* systems. There is therefore a strong need for *in vivo* model systems that allow these interactions to be studied in detail at the cellular as well as the genomic and proteomic level. Such models will also be important for the development of new therapeutic intervention strategies targeting cancer.

Ideally, such models should allow a complete separation of the tumor-host cellular compartments for further analysis. However, because of the extensive cellular heterogeneity within tumors, it is extremely difficult to separate tumor and host cells based on specific phenotypic markers. Therefore, color-coded tumor host model systems have been developed that offer the possibility of imaging tumor-host interactions at the cellular level, and a number of tumor cell lines have been used for this purpose (10–13). In the present work, we have generated a novel NOD/Scid (nonobese-diabetic/severe combined immunodeficient) transgenic mouse ubiquitously expressing enhanced green fluorescent protein (eGFP) in all nucleated cells, a strain that is deficient in both the adaptive and innate immune system. NOD/Scid mice lack B and T lymphocytes and have low natural killer (NK) cell and hemolytic complement activity, defects in myeloid development, and poor antigen-presenting-cell function (14). These mice allow a higher percentage of engraftment

[1] Correspondence: CRP-Santé, NorLux Neuro-Oncology Laboratory, 84, Val Fleuri, L-1526 Luxembourg. E-mail: simone.niclou@crp-sante.lu

doi: 10.1096/fj.08-109611

0892-6638/08/0022-3120 © The Author(s)

compared to nude mice (15) and represent an advanced model for long-term xeno-engraftment studies. We have characterized the mice in detail at the immunological level and show that they allow the growth of a variety of tumor types (both subcutaneously and orthotopically), including tumors stably expressing fluorescent marker proteins. We show how the tumor and host cells can be visualized *in situ* using advanced imaging techniques and how the tumor-host cellular compartments can be phenotyped and completely separated for further genomic and proteomic analyses. Finally, we present evidence that the method can be used to determine tumor-host cell fusion events thus providing a tool to study cellular hybrids generated during tumor progression (16).

MATERIALS AND METHODS

Animals

eGFP-expressing NOD/Scid mice were generated by crossing NOD.CB17.Prkdc^{scid} mice (stock no. 003291) with C57BL/6-Tg (ActB eGFP) mice (stock no. 001303) (Jackson Laboratory, Bar Harbor, ME, USA). eGFP cDNA under the control of the chicken beta-actin promoter and cytomegalovirus enhancer results in GFP expression in all nucleated cells. Breedings were performed between heterozygous eGFP and homozygous NOD.CB17-*Prkdc^{scid}* genotyped by polymerase chain reaction (PCR) analysis (Supplemental Results; Supplemental Fig. 1*A*). Transplantation experiments were performed with mice at 3 or 4 generations. At present, backcrossing to the parental NOD/Scid background to obtain a congenic line is ongoing.

Flow cytometry

Immunophenotyping was performed by 6-color multiparameter flow cytometry on peripheral blood and splenocytes obtained from eGFP-expressing NOD/Scid mice and from immunocompetent C57BL/6 mice. The following markers were assessed: CD3, CD4, CD8, CD11c, CD14, CD19, CD34, CD45, GR-1, DX5 (CD49b), and NK1.1 (Supplemental Materials and Methods). Analyses were performed using a FACS Canto flow cytometer (Becton Dickinson, Erembodegem, Belgium).

Tumor cultures

A number of human glioma cell lines (U87, U251, U373) and murine cancer cell lines were studied, including four mammary tumors (C3HBA, H2712, MA13C, and MA16C), three fibrosarcomas (FBSARB, KHT-1, and FBSARA) and one squamous cell carcinoma (SCCVII) (Supplemental Materials and Methods). Some cell lines were stably transfected with red fluorescent protein using a dsRed-expressing lentiviral vector (Supplemental Materials and Methods). Human brain tumor biopsies (glioblastoma multiforme) were obtained from the Department of Neurosurgery, Centre Hospitalier, Luxembourg City, Luxembourg. Collection of tumor tissue was approved by the ethical committee in Luxembourg (CNER). Biopsy spheroids were prepared as described previously (17). Briefly, tissue samples were minced into 0.5-mm fragments and cultured in agar-coated tissue culture flasks in complete culture medium. The spheroids were maintained in a standard tissue culture incubator with 5% CO_2 in air and 100% relative humidity at 37°C, and the medium was changed once a week. After 2 wk in culture, spheroids with diameters between 200 and 300 μm were selected for intracerebral implantation. All cell cultures were performed using Dulbecco modified Eagle medium (DMEM) containing 10% fetal calf serum (FCS) supplemented with nonessential amino acids (NEAA), 100 U/ml Pen/Strep, and 400 μM L-glutamine, all from Cambrex (Lonza, Switzerland).

In vivo experiments

Subcutaneous tumors were established by injection of a cell suspension (5×10^6 cells in 100 μl PBS) into the flank or neck of 6- to 10-wk-old mice. Tumor development was generally visible within 2–4 wk, depending on the cell line injected (**Fig. 2*A***; Supplemental Table 1). Subcutaneous tumor growth was measured at regular intervals using vernier calipers. Tumor volume was calculated using the formula $a^2b/2$, where a and b are the shorter and longer diameter of the tumor, respectively. For brain implantations, mice were anesthetized with a mixture of ketamine (10 mg/ml) and xylazine (1 mg/ml) and fixed in a stereotactic frame (Narishige Group, Tokyo, Japan), and a small hole was drilled in the skull. Tumor spheroids (5–6/mouse) or tumor cell suspension (2 μl, corresponding to 2×10^5 cells) were slowly injected through a Hamilton syringe (Hamilton, Reno, NV, USA) into the right frontal cortex. Development of tumors from cell lines took 2–4 wk, whereas the tumors that developed from primary biopsies (tumor spheroids) took 5–6 months. All animals were fed a standard pellet diet and provided water *ad libitum*. All procedures were approved by the National Animal Research Authority in Luxembourg. The brains from animals bearing primary brain tumor transplants were carefully dissected out, and new biopsy spheroids were generated. The spheroids were then seeded on a plastic surface and studied *ex vivo* using a fluorescence microscope (Leica DMI 6000B; Leica Microsystems, Wetzlar, Germany).

Microscopy

Fluorescence and brightfield microscopy

Direct GFP and dsRed fluorescence was observed on paraformaldehyde-fixed cryostat sections. Immunostaining for mouse endothelial cells was carried out on fresh-frozen acetone-fixed sections (where endogenous GFP and DsRed fluorescence is lost) with a rat anti-mouse CD31 [platelet/endothelial cell adhesion molecule (PECAM)] antibody (CBL1337; Chemicon, Biognost, Heule, Belgium), visualized with an anti-rat Alexa Fluor 647 secondary antibody (Invitrogen, Merelbeke, Belgium) (**Fig. 3*C***). In these sections, tumor cells were counterstained with a human-specific antibody (anti-vimentin MAB3400; Chemicon) detected with an Alexa Fluor 488 coupled secondary antibody (Invitrogen) (Fig. 3*C*). Sections were counterstained with 4′,6′-diamidino-2-phenylindole (DAPI). Histology (Fig. 2*D*) was done on brains fixed in formaline and embedded in paraffin; sections were stained with standard hematoxylin and eosin (H&E) procedures. Fluorescent and brightfield images were obtained using a Leica DMI 6000B microscope using a DFC350 camera and the LAS software (Leica Microsystems).

Multiphoton microscopy

The tumors were visualized *in situ* using a Leica SP5 multiphoton confocal microscope equipped with a Coherent Chameleon-Ultratuning range 690-1040 nm laser (Leica Microsys-

tems). 30 slices were obtained from a depth of 150 μm (Fig. 3*E*). The images were further analyzed using three-dimensional Imaris imaging visualization software (Bitplane AG, Zurich, Switzerland).

Cell sorting

Freshly isolated U87 tumors were dissociated by mincing the tissue with scalpels, followed by incubation in HBSS-containing collagenase for 30 min at 37°C. Incompletely dissociated tissue was digested a second time. The cell suspension was triturated in the presence of DNase I and filtered through a 100-μm cell strainer.

The cells were resuspended in PBS and sorted on a fluorescence-activated cell sorter (FACS Aria SORP, BD Biosciences, Erembodegem, Belgium) on the basis of single-cell viability and the presence of GFP and DsRed. After isolation from the green mice, we observed that tumor cells showed some green fluorescence. This was the case for unlabeled cells (not shown) or DsRed-labeled tumor cells (rectangle in **Fig. 4**). However, these cells are not truly double positive when viewed under the microscope and are still clearly separated from green host cells. For immunophenotyping, cells were incubated with labeled antibodies prior to FACS analysis (Supplemental Materials and Methods).

RESULTS

Characterization of NOD/Scid eGFP-expressing mice

To obtain a homozygous NOD/Scid mouse expressing eGFP (**Fig. 1*A***), the NOD.CB17.Prkdc^{scid} strain was crossed with the C57BL/6-Tg (ActB-eGFP) strain (18) for several generations. The animals were routinely tested by PCR for eGFP expression stability and NOD/Scid status (Supplemental Fig. 1*A*). Moreover, using a UV dissecting microscope, eGFP expression in all internal organs was determined. Besides erythrocytes and fat, all internal organs displayed strong eGFP expression (Fig. 1*B*). A proportion (7%) of the eGFP-expressing animals had extremely small bodies, attaining a body weight of only 50% of that of ordinary NOD/Scid mice. These animals were strongly fluorescent and died between 6 and 10 wk, which has also been reported for the eGFP-expressing parental strain (18).

We next investigated whether NOD/Scid eGFP mice had the same immunological deficits as the parental NOD/Scid line. Peripheral blood was incubated with antibodies against specific marker proteins of the hematopoietic system and analyzed by 6-color flow cytometry (Fig. 1*C*). There was no difference in immune status between the NOD/Scid eGFP line and their non-eGFP counterparts. Quantification revealed a strong and stable reduction of B and T lymphocytes (Supplemental Fig. 1*C, D*). Although a relatively high percentage of DX5$^+$ cells is present in NOD/Scid eGFP mice (Fig. 1*C* and Supplemental Fig. 1*C*), little or no NK cell activity was detected in these mice (Supplemental Fig. 1*E*), as is expected for the NOD/Scid strain (14). The same immunological profile was observed in splenocytes of these mice (data not shown).

Tumor growth

A range of mouse and human tumor cell lines (glioma, breast cancer, fibrosarcoma, squamous cell carcinoma) with or without DsRed expression were transplanted subcutaneously (s.c.) in the flank or in the neck of the animals. Also, human brain tumors (cell lines as well as biopsy spheroids) were transplanted orthotopically in the brain. The tumor take rate was close to 100% in the NOD/Scid eGFP mice for all the assessed tumors (Supplemental Table 1). Interestingly, for several tumor lines, the take rate was even higher in the NOD/Scid eGFP animals than in syngeneic C3H mice (Supplemental Table 1). No differences in tumor growth were seen between NOD/Scid and NOD/Scid eGFP mice, indicating that eGFP expression in the host did not affect tumor growth (**Fig. 2*A***). Correspondingly, when wild-type tumors were compared to their dsRed-expressing counterparts, we observed a similar growth rate, indicating that dsRed expression did not affect tumor growth (Fig. 2*B*).

We also implanted a human dsRed-expressing glioma line (U87 dsRed), as well as glioblastoma biopsy spheroids in the brain. As expected, the cell line showed a well-circumscribed tumor growth within the brain (Fig. 2*C*). We have earlier shown that highly infiltrative brain tumors with a stemlike phenotype can be established by xenotransplantation of human glioblastoma biopsy spheroids in immunodeficient nude rats (19). These tumors coopt the host vasculature and present as an aggressive disease without signs of angiogenesis (19). To determine whether the same phenotype could be established, we performed similar transplantation experiments in the brains of NOD/Scid eGFP mice (*i.e.*, stereotactic transplantation of 6 human glioblastoma biopsy spheroids into the frontal cortex). Tumor take rate for the xenotransplants was 100% (Supplemental Table 1). Also in these animals, a highly infiltrative phenotype was observed, with tumor cells invading the white matter tracts (Fig. 2*D*).

Visualization of tumor host cellular interactions *ex vivo*

The human brain tumors depicted in Fig. 2*D* were removed from the mouse brain, and new biopsy spheroids were established (17). These spheroids were allowed to attach to a plastic surface and were observed by fluorescence light and confocal microscopy. As shown in Fig. 2*E*, the host cells were readily visible within the tumor spheroids, allowing a further characterization of tumor-host cellular interactions *ex vivo*, using the cells that have established a natural relationship *in vivo*. Some of the eGFP-expressing cells showed stem cell-like characteristics, adopting a differentiated phenotype under serum conditions (Fig. 2*E*, inset). Moreover, in addition to multinucleated tumor cells, a small population of multinucleated eGFP-expressing cells was observed (Fig. 2*F*). These may result from incomplete cell division or cell fusion events, although

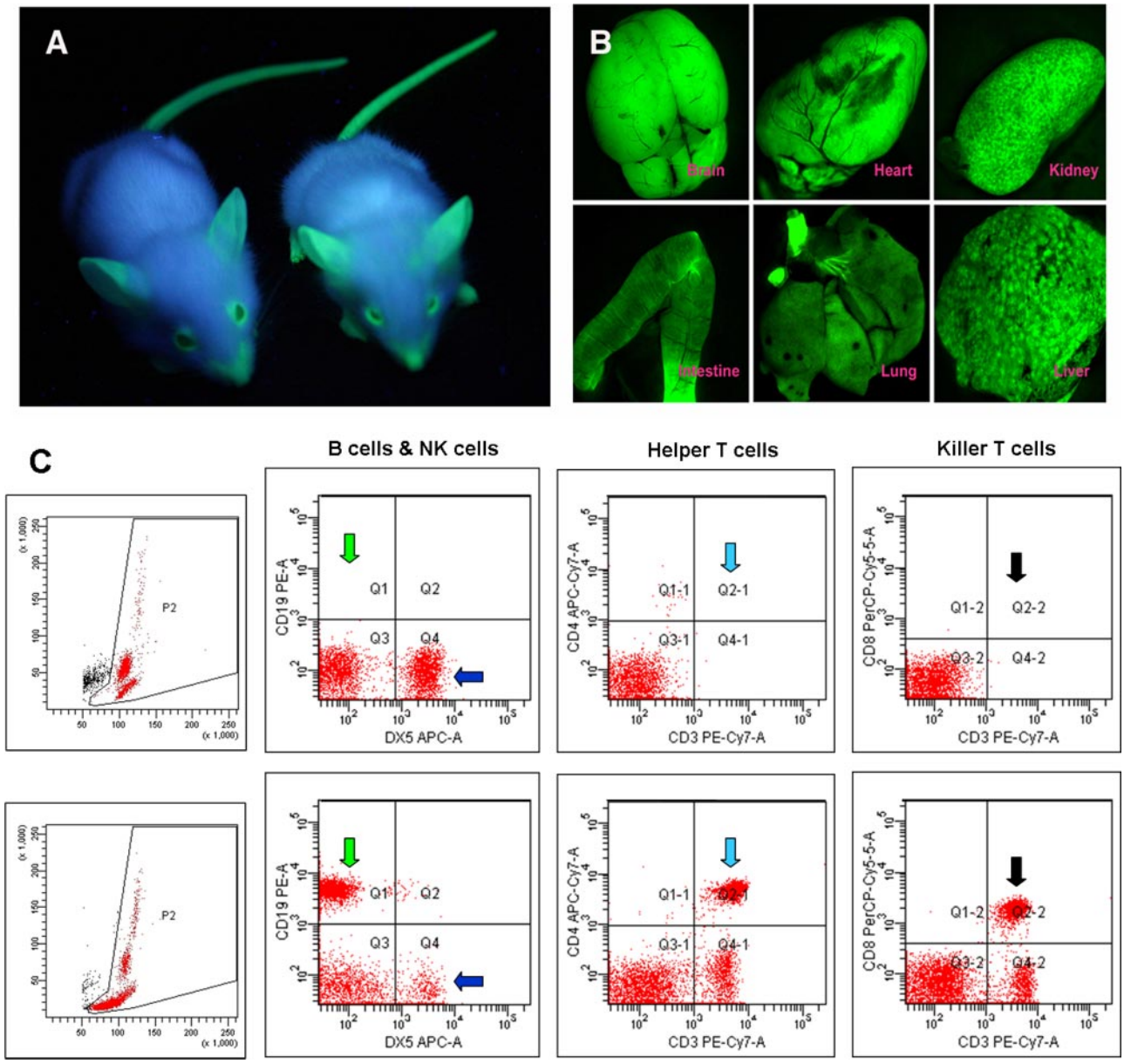

Figure 1. *A*) NOD/Scid eGFP mice visualized under a handheld UV lamp. *B*) Internal organs showing strong eGFP expression in brain, heart, kidney, intestine, lung, and liver under a fluorescence dissecting microscope. *C*) Flow cytometric immunophenotyping of blood of NOD/Scid eGFP mice (top panels) and C57BL/6 immunocompetent mice (bottom panels), showing almost complete absence of $CD19^+$ B cells (green arrows), $CD3^+/CD4^+$ T cells (light blue arrows), and $CD3^+/CD8^+$ T cells (black arrows) in NOD/Scid eGFP mice, and a relative increase in $DX5^+$ natural killer (NK) cells (dark blue arrows). Left panels show the respective forward scatter (*x* axis) *vs.* side scatter (*y* axis) dot plots, also revealing the lack of major cell populations in NOD/Scid eGFP mouse blood (top).

further analysis at the DNA level is necessary to support this.

Visualization of the tumor angioarchitecture

Using a dissecting microscope with UV-filter optics for dsRed and eGFP, a detailed macroscopic outline of a subcutaneous tumor (red) and host tissue (green) was observed (**Fig. 3*A***). Interestingly, the overall tumor surface angioarchitecture was readily visualized, as the blood vessels within the tumor bed appeared darker, due to the fact that red blood cells do not express eGFP. Direct fluorescence in histological sections enabled us to readily visualize eGFP-expressing host cells within the tumor bed (Fig. 3*B*). A large proportion of these appeared to be endothelial cells, as shown by mouse-specific CD31 (PECAM) staining (Fig. 3*C*). However, in some tumor areas, an eGFP-expressing endothelial lining was not evident, suggesting the occurrence of vasculogenic mimicry (Fig. 3*D*). Next, we used multiphoton confocal microscopy to further analyze the tumor-host cellular compartments in the living mouse. By this technology, we were able to visualize in three dimensions the

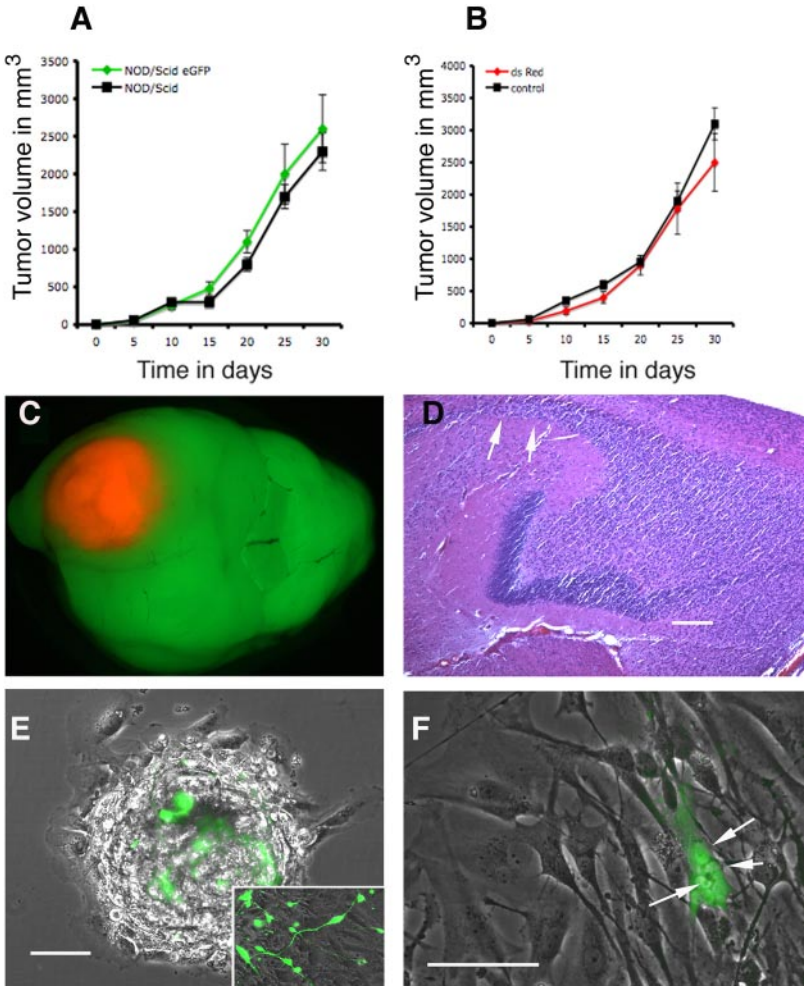

Figure 2. A) U87 subcutaneous tumor growth in NOD/Scid eGFP and in NOD/Scid mice show the same growth rate, indicating that eGFP expression did not affect tumor growth (see also Supplemental Table 1). *B*) Growth of U87 DsRed$^+$ tumors compared to U87 control cell line, indicating that dsRed also did not affect tumor growth (see also Supplemental Table 1). *C*) Direct fluorescence of a U87 dsRed tumor grown orthotopically in the brain and visualized under a fluorescence dissecting microscope. *D*) Histology of a highly infiltrative human glioblastoma xenotransplant in the brain of NOD/Scid eGFP mice (5 months after transplantation). Note the invading tumor cells (white arrows) within the hippocampus and along white matter tracts. *E*) Biopsy spheroids initiated from the glioblastoma xenotransplant depicted in *D* were generated and seeded on a plastic surface, allowing a further characterization of tumor-host cellular interactions *ex vivo* of cells that have established a natural relationship *in vivo*. Inset shows eGFP-expressing cells that appear to differentiate on serum withdrawal. *F*) A small population of multinucleated eGFP-expressing cells was observed. Growth curves: mean ± SE, $n = 5$. Scale bars = 200 μm (*D*, *E*); 100 μm (*F*).

tumor cells and host cells *in situ* (Fig. 3*E*). Moreover, using advanced visualization software and three-dimensional image reconstruction, the tumor-host compartment within a certain volume could be quantified (Fig. 3*E*, inset).

Separation and phenotyping of the host cellular compartment

The tumors were removed from the mice and enzymatically dissociated into a single-cell suspension. The green and red cells were sorted using a high-speed FACS, which allowed us to exactly quantify the percentage of host and tumor cells within the tumors (**Fig. 4**). The percentage of stromal cells varied between 4 and 6% for subcutaneous and brain tumors. Moreover, the sorting procedures allowed a pure collection of host and tumor cells that could be further characterized at the genomic and proteomic level. Using cell-type specific markers, we were able to detect the following marker proteins, suggesting the presence of the indicated cell types within the host cell compartment: endothelial cells (CD31$^+$), fibroblasts and/or mesenchymal stem cells (CD90$^+$), natural killer cells (DX5$^+$), monocyte/macrophage lineage (CD14$^+$), and dendritic cells (CD11c$^+$). As expected, marker expression was found on normal (host) cells but little on tumor cells (Fig. 4 quantification data).

Confirming the light microscopic observations, we were also able to identify a small proportion of green and red double-positive cells within the tumors. Interestingly some of these cells were multinucleated (**Fig. 5**), again suggesting the occurrence of cell fusion or horizontal gene transfer in tumors. Thus, a further characterization of such cells will provide valuable information related to a long-debated controversy, that is, to what extent do cell fusion or horizontal gene transfer events contribute to tumor initiation and progression (20–22).

DISCUSSION

Cancer research is highly dependent on reliable animal models that allow the study of different aspects of cancer initiation and progression *in vivo*. For xenotransplantation experiments, the research community relies on immunodeficient animals, such as the nude rats and mice, the Rag mutants, or the NOD/Scid mutants (23, 24). In the present work, we have developed and characterized an eGFP-expressing NOD/Scid mouse showing ubiquitous eGFP expression. The im-

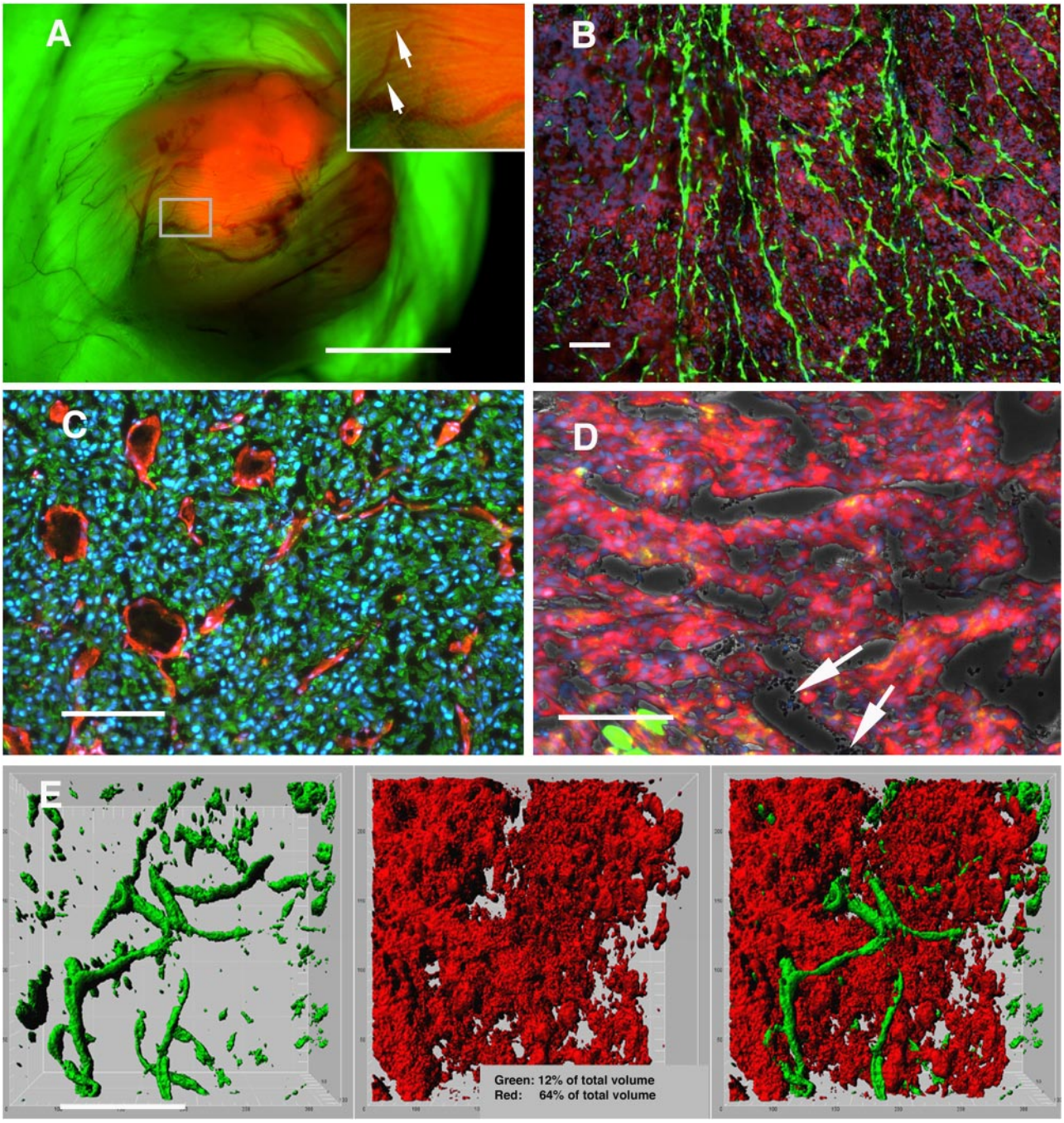

Figure 3. *A*) *In situ* picture of a U373 dsRed tumor growing s.c. in the NOD/Scid eGFP mouse, after removal of the skin flap. Note the detailed visualization of blood vessels. Also, a thin layer of striated muscle fibers is seen covering the tumor (inset, arrows). The picture was taken using a fluorescence dissecting microscope. *B*) Endogenous fluorescence on a frozen histological section from a U87 subcutaneous tumor showing eGFP-expressing host cells within the tumor bed (direct eGFP and dsRed fluorescence, counterstained with DAPI). *C*) Identification of mouse endothelial cells in the tumor bed by mouse-specific CD31 immunostaining (red). Here, tumor cells were counterstained with a human-specific antibody (vimentin; green), because endogenous fluorescence of GFP and dsRed is lost on acetone fixation. *D*) In some tumor areas, an eGFP-expressing endothelial lining was not evident, yet erythrocytes were present in the lumen (arrows), reminiscent of vasculogenic mimicry. Picture taken from a U87 tumor grown s.c. *E*) Visualization of a U251 tumor *in situ* using a Leica SP5 multiphoton confocal microscope at a depth of 150 μm. Three-dimensional reconstructions of 30 slices analyzed using three-dimensional Imaris imaging software allowed the quantification of tumor *vs.* host cell volume. Pictures show the green and red channels separately and merged. Scale bars = 7 mm (*A*); 100 μm (*B*); 200 μm (*C–E*).

munological profile of NOD/Scid eGFP mice was comparable to that of the nontransgenic parental line. Tumor take and progression were also unchanged between the two lines. These mice accept a high proportion of allogeneic and xenogeneic transplants and represent an ideal model to address important questions related to cancer and immunology research. With more refined research questions addressed, the

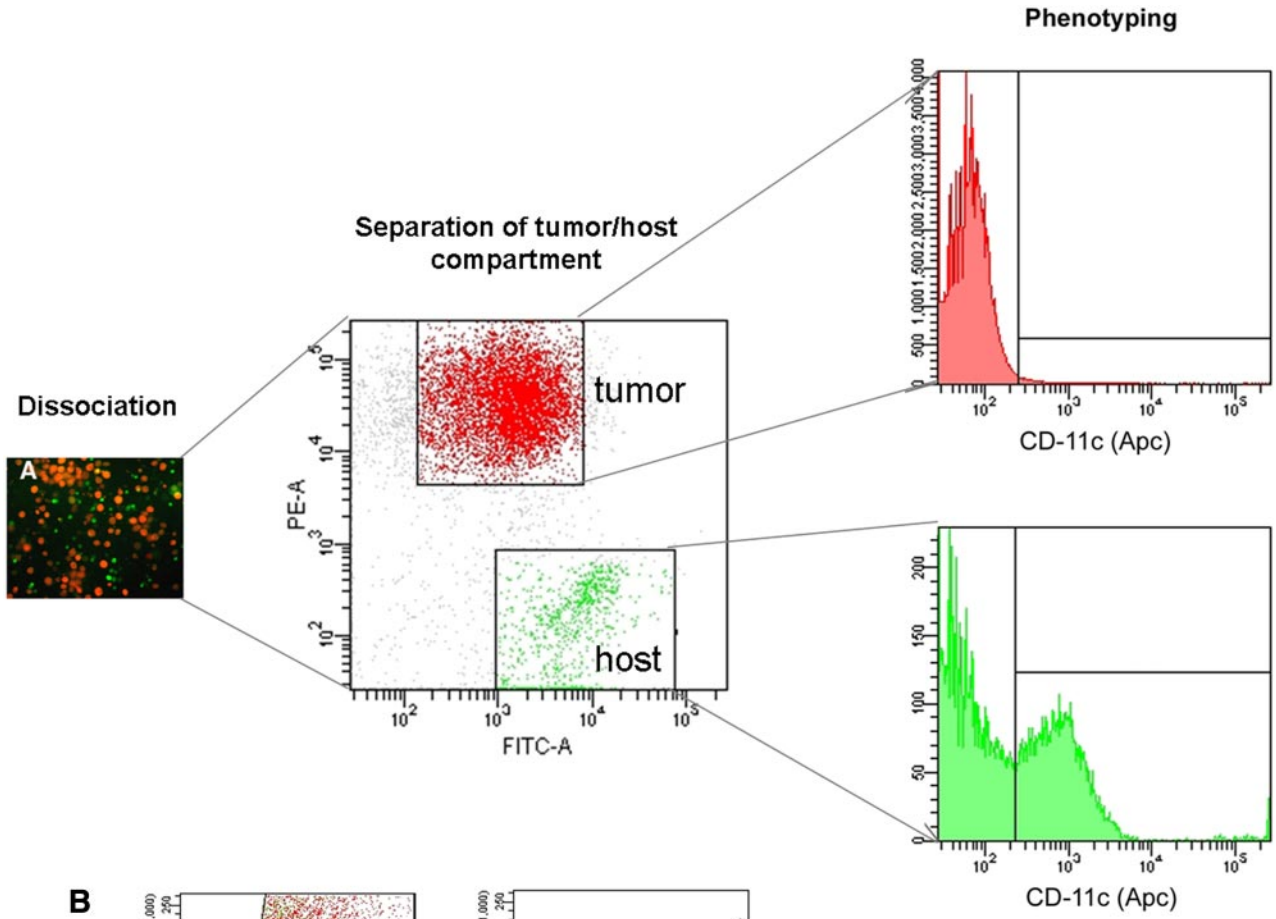

B

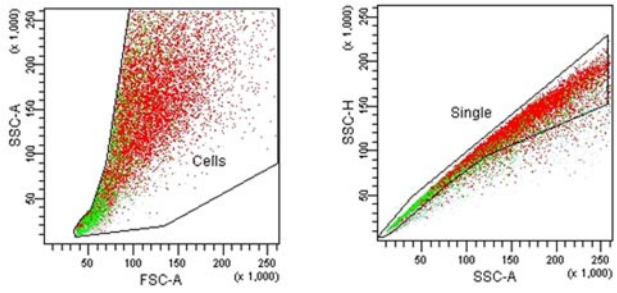

C

Quantification of phenotypic markers in tumor cells and host cells (s.c U87 tumor)*

Antibody	Specificity	% Positive host cells (green)[1]	%Positive tumor cells (red)
CD31	endothelial cells	4.6	0.3
CD90	fibroblasts and MSC[2]	12.1	2.6
CD49b(DX5)	Natural Killer cells (NK)	16.9	1.7
CD14	monocyte/macrophage	34.7	1.8
CD11c	dendritic cells	32.2	1.3

* Representative data from two experiments
1) 4% the total cell population was host derived (green).
2) Mesenchymal stem cells (MSC)

Figure 4. Flow cytometric separation, phenotyping, and quantification of the tumor and host cellular compartments from a DsRed-expressing U87 tumor grown in a NOD/Scid eGFP mouse. *A*) The tissue was dissociated into a single-cell suspension, which was separated and phenotyped using different markers. As expected, several immune cell markers (*e.g.*, CD11c for dendritic cells) are found within the host cell population but not within the tumor cell population. *B*) Gates applied in the flow cytometric analysis to remove cell debris and doublets prior to sorting. *C*) Quantification table of the markers applied.

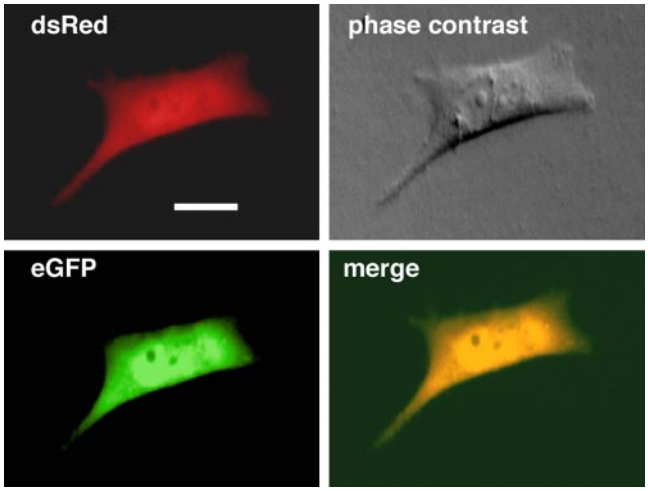

Figure 5. Sorted cells from a U87 DsRed tumor showing both red and green fluorescence, suggesting cell fusion or horizontal gene transfer events. Scale bar = 15 μm.

demand on the number, diversity, and specialized research applications of immunodeficient animal models will increase. The previously described eGFP-expressing nude mouse (11) is particularly useful for *in vivo* imaging of tumor cells due to its hairless phenotype (12). The NOD/Scid eGFP mouse represents an advanced animal model for long-term xenotransplantation studies with primary human biopsies. Compared to other immunodeficient mutants, the model supports enhanced engraftment of allogeneic and xenogeneic cells, tissues, and tumors, as well as reconstitution of the hematopoietic system after bone marrow transplantation (23). In addition, the strain is well characterized, breeds well, and displays very low immunological leakiness with age (24).

Research applications

Supporting previous reports in eGFP-expressing nude mice, we show that the tumor and the host tissue can be studied in detail both *in situ* and *ex vivo*. We further show by using multiphoton confocal microscopy that the number of vascular elements, tumor cells, and normal cells can be visualized and quantified in detail. The tumor model can be used to detect and quantify vasculogenic mimicry within tumors—a phenomenon that has been highly debated during recent years (25, 26). We also show that the dsRed-expressing tumors can be dissociated into a single-cell suspension yielding red and green cells. By using multiparameter flow cytometric techniques, we were able to show that precise phenotyping of the host cellular compartment is possible (Fig. 4*C*). Additional cell markers need to be applied to reveal the exact nature of the stromal cells. Thus, multiparameter cell-sorting techniques together with genomic and proteomic analyses should provide valuable information on how individual normal cell types change within tumors, for instance during tumor progression and as a response to treatment. Similarly, using flow cytometric analyses of blood and lymph nodes, it should be possible to detect, separate, and phenotype circulating tumor cells, as well as metastatic tumor cells in lymph nodes.

We further show for the first time the presence of multinucleated double-positive cells within tumors that were isolated in the flow cytometric analyses and in *ex vivo* experiments. These cells are likely to be derived from cell fusion or horizontal gene transfer events, although further analysis on the DNA level is required to support this view. Arguably, such cells deserve further analysis with regard to their growth potential and tumorigenicity *in vivo*.

Although not addressed in the present work, the model may also be used to study the involvement of stem cells in tumor development. Tissue-specific stem cells and mesenchymal stem cells have been shown to migrate into tumors (27, 28). A future challenge is to elucidate their contribution to tumor development. Because stem cells are prone to oncogenic insults or may be influenced by tumor cells, stem cells may play a role in tumor development and progression. Alternatively, stem cells may fuse to tumor cells and thereby gain genomic instability (20).

In conclusion, we present here proof of concept for a wide range of experimental applications and performance of the NOD/Scid eGFP-expressing mouse model. Thus, a tool has been developed that allows for a detailed genomic and proteomic profiling of specific host cells within the tumors. Moreover, our model system enables detailed studies on the vascular compartments within tumors, including vasculogenic mimicry. The model can also be used for the detection of double-positive cells arising from cell fusion and horizontal gene transfer events and should provide significant insight into the role of such cells in tumor progression. Further in-depth analysis is needed to explore such complicated phenomena. In addition to the described applications in cancer research, NOD/Scid eGFP mice will be invaluable for the study of the immune system and as hosts for infectious agents (29). FJ

This work was supported by the Norwegian Cancer Society; the Norwegian Research Council; Innovest AS; the Western Norway Regional Health Authority; Haukeland University Hospital, Bergen, Norway; The Bergen Translational Research Programme; the Centre de Recherche Public de la Santé (CRP-Santé) through a grant from the Research Ministry in Luxembourg; and the European Commission 6th Framework Program (contract 504743). The technical assistance of Vanessa Barthelemy, Virginie Baus, and Lene Nybø is greatly appreciated.

REFERENCES

1. Kalluri, R., and Zeisberg, M. (2006) Fibroblasts in cancer. *Nat. Rev. Cancer* **6,** 392–401
2. Langley, R. R., and Fidler, I. J. (2007) Tumor cell-organ microenvironment interactions in the pathogenesis of cancer metastasis. *Endocrine Rev.* **28,** 297–321

3. Axelrod, R., Axelrod, D. E., and Pienta, K. J. (2006) Evolution of cooperation among tumor cells. *Proc. Natl. Acad. Sci. U. S. A.* **103,** 13474–13479
4. Koebel, C. M., Vermi, W., Swann, J. B., Zerafa, N., Rodig, S. J., Old, L. J., Smyth, M. J., and Schreiber, R. D. (2007) Adaptive immunity maintains occult cancer in an equilibrium state. *Nature* **450,** 903–907
5. Aguirre-Ghiso, J. A. (2007) Models, mechanisms and clinical evidence for cancer dormancy. *Nat. Rev. Cancer* **7,** 834–846
6. Ben-Baruch, A. (2006) The multifaceted roles of chemokines in malignancy. *Cancer Metastasis Rev.* **25,** 357–371
7. Bierie, B., and Moses, H. L. (2006) Tumour microenvironment: TGFβ: the molecular Jekyll and Hyde of cancer. *Nat. Rev. Cancer* **6,** 506–520
8. Munshi, H. G., and Stack, M. S. (2006) Reciprocal interactions between adhesion receptor signaling and MMP regulation. *Cancer Metastasis Rev.* **25,** 45–56
9. Stamenkovic, I. (2003) Extracellular matrix remodelling: the role of matrix metalloproteinases. *J. Pathol.* **200,** 448–464
10. Yang, M., Li, L., Jiang, P., Moossa, A. R., Penman, S., and Hoffman, R. M. (2003) Dual-color fluorescence imaging distinguishes tumor cells from induced host angiogenic vessels and stromal cells. *Proc. Natl. Acad. Sci. U. S. A.* **100,** 14259–14262
11. Yang, M., Reynoso, J., Jiang, P., Li, L., Moossa, A. R., and Hoffman, R. M. (2004) Transgenic nude mouse with ubiquitous green fluorescent protein expression as a host for human tumors. *Cancer Res.* **64,** 8651–8656
12. Hoffman, R. M., and Yang, M. (2006) Whole-body imaging with fluorescent proteins. *Nat. Protoc.* **1,** 1429–1438
13. Glinsky, G. V., Glinskii, A. B., Berezovskaya, O., Smith, B. A., Jiang, P., Li, X. M., Yang, M., and Hoffman, R. M. (2006) Dual-color-coded imaging of viable circulating prostate carcinoma cells reveals genetic exchange between tumor cells in vivo, contributing to highly metastatic phenotypes. *Cell Cycle* **5,** 191–197
14. Shultz, L. D., Schweitzer, P. A., Christianson, S. W., Gott, B., Schweitzer, I. B., Tennent, B., McKenna, S., Mobraaten, L., Rajan, T. V., Greiner, D. L., and Leiter, E. H. (1995) Multiple defects in innate and adaptive immunologic function in NOD/LtSz-scid mice. *J. Immunol.* **154,** 180–191
15. The Jackson Laboratory (1999) An improved scid mouse for cancer and immunological research. *JAX Notes* **476.** http://jaxmice.jax.org/jaxnotes/archive/476b.html
16. Bjerkvig, R., Tysnes, B. B., Aboody, K. S., Najbauer, J., and Terzis, A. J. (2005) Opinion: the origin of the cancer stem cell: current controversies and new insights. *Nat. Rev. Cancer* **5,** 899–904
17. Bjerkvig, R., Tonnesen, A., Laerum, O. D., and Backlund, E. O. (1990) Multicellular tumor spheroids from human gliomas maintained in organ culture. *J. Neurosurg.* **72,** 463–475
18. Okabe, M., Ikawa, M., Kominami, K., Nakanishi, T., and Nishimune, Y. (1997) 'Green mice' as a source of ubiquitous green cells. *FEBS Lett.* **407,** 313–319
19. Sakariassen, P. O., Prestegarden, L., Wang, J., Skaftnesmo, K. O., Mahesparan, R., Molthoff, C., Sminia, P., Sundlisaeter, E., Misra, A., Tysnes, B. B., Chekenya, M., Peters, H., Lende, G., Kalland, K. H., Oyan, A. M., Petersen, K., Jonassen, I., van der Kogel, A., Feuerstein, B. G., Terzis, A. J., Bjerkvig, R., and Enger, P. O. (2006) Angiogenesis-independent tumor growth mediated by stem-like cancer cells. *Proc. Natl. Acad. Sci. U. S. A.* **103,** 16466–16471
20. Tysnes, B. B., and Bjerkvig, R. (2007) Cancer initiation and progression: involvement of stem cells and the microenvironment. *Biochim. Biophys. Acta* **1775,** 283–297
21. Duelli, D., and Lazebnik, Y. (2007) Cell-to-cell fusion as a link between viruses and cancer. *Nat. Rev. Cancer* **7,** 968–976
22. Holmgren, L., Bergsmedh, A., and Spetz, A. L. (2002) Horizontal transfer of DNA by the uptake of apoptotic bodies. *Vox Sang.* **83**(Suppl. 1), 305–306
23. Greiner, D. L., Hesselton, R. A., and Shultz, L. D. (1998) SCID mouse models of human stem cell engraftment. *Stem Cells* **16,** 166–177
24. The Jackson Laboratory (2006) Choosing an immunodeficient mouse model. *JAX Notes* **501.** http://jaxmice.jax.org/jaxnotes/archive/501a.html
25. Hillen, F., and Griffioen, A. W. (2007) Tumour vascularization: sprouting angiogenesis and beyond. *Cancer Metastasis Rev.* **26,** 489–502
26. Hendrix, M. J., Seftor, E. A., Hess, A. R., and Seftor, R. E. (2003) Vasculogenic mimicry and tumour-cell plasticity: lessons from melanoma. *Nat. Rev. Cancer* **3,** 411–421
27. Aboody, K. S., Brown, A., Rainov, N. G., Bower, K. A., Liu, S., Yang, W., Small, J. E., Herrlinger, U., Ourednik, V., Black, P. M., Breakefield, X. O., and Snyder, E. Y. (2000) Neural stem cells display extensive tropism for pathology in adult brain: evidence from intracranial gliomas. *Proc. Natl. Acad. Sci. U. S. A.* **97,** 12846–12851
28. Nakamizo, A., Marini, F., Amano, T., Khan, A., Studeny, M., Gumin, J., Chen, J., Hentschel, S., Vecil, G., Dembinski, J., Andreeff, M., and Lang, F. F. (2005) Human bone marrow-derived mesenchymal stem cells in the treatment of gliomas. *Cancer Res.* **65,** 3307–3318
29. Greiner, D. L., Rajan, T. V., and Shultz, L. D. (1992) Animal models for immunodeficiency diseases. *Immunol. Today* **13,** 116–117

Received for publication March 12, 2008.
Accepted for publication April 24, 2008.